G359.87+0.18, AN FR II RADIO GALAXY 15' FROM SAGITTARIUS A*: IMPLICATIONS FOR THE SCATTERING REGION IN THE GALACTIC CENTER

T. JOSEPH W. LAZIO[1]

NRL, Code 7210, Washington, DC 20375-5351; lazio@rsd.nrl.navy.mil

K. R. ANANTHARAMAIAH[2] AND W. M. GOSS

NRAO, P. O. Box 0, Socorro, NM 87801; anantha@aoc.nrao.edu; mgoss@nrao.edu

NAMIR E. KASSIM

NRL, Code 7213, Washington, DC, 20375-5351; nkassim@rsd.nrl.navy.mil

AND

JAMES M. CORDES

Department of Astronomy, Cornell University and NAIC, 520 Space Sciences Building, Ithaca, NY 14853-6801; cordes@spacenet.tn.cornell.edu

Received 1998 August 11; accepted 1998 November 18

ABSTRACT

G359.87+0.18 is an enigmatic object located 15' from Sgr A*. It has been variously classified as an extragalactic source, a Galactic jet source, and a young supernova remnant. We present new observations of G359.87+0.18 between 0.33 and 15 GHz and an H I absorption spectrum and use these to argue that this source is an FR II radio galaxy. We are able to place a crude limit on its redshift of $z \gtrsim 0.1$. The source has a spectral index of $\alpha < -1$ ($S \propto v^\alpha$), suggestive of a radio galaxy with a redshift $z \gtrsim 2$. The scattering diameters of Sgr A* and several nearby OH masers ($\approx 1''$ at 1 GHz) indicate that a region of enhanced scattering is along the line of sight to the Galactic center. If the region covers the Galactic center uniformly, the implied diameter for a background source is at least $600''$ at 0.33 GHz, which is in contrast with the observed $20''$ diameter of G359.87+0.18. Using the scattering diameter of a nearby OH maser OH 359.762+0.120 and the widths of two nearby nonthermal threads, G0.08+0.15 and G359.79+0.17, we show that a uniform scattering region should cover G359.87+0.18. We therefore conclude that the Galactic center scattering region is inhomogeneous on a scale of 5' (≈ 10 pc at a distance of 8.5 kpc). This scale is comparable with the size scale of molecular clouds in the Galactic center. The close agreement between these two length scales is an indication that the scattering region is linked intimately to the Galactic center molecular clouds.

Subject headings: galaxies: individual (G359.87+0.18) — Galaxy: center — radio continuum: galaxies — scattering

1. INTRODUCTION

The observed diameter of Sgr A*, the compact source in the Galactic center (GC), scales as λ^2, as is expected if interstellar scattering from microstructure in the electron density determines the observed diameter (Davies, Walsh, & Booth 1976). The observed diameter of Sgr A* is now known to scale as λ^2 from 30 cm to 3 mm and to be anisotropic at least over the wavelength range 21 cm to 7 mm (Backer et al. 1993; Krichbaum et al. 1993; Rogers et al. 1994; Yusef-Zadeh et al. 1994; Bower & Backer 1998). Maser spots in OH/IR stars within 25' of Sgr A* also show enhanced, anisotropic angular broadening (van Langevelde et al. 1992; Frail et al. 1994). These observations indicate that a region of enhanced scattering with an angular extent of at least 25' in radius (60 pc at 8.5 kpc) is along the line of sight to the GC. Assuming that the region covers the GC uniformly, the scattering diameter of an extragalactic source seen through this region should be larger than those of Galactic sources by the ratio D_{GC}/Δ_{GC}, where D_{GC} is the Sun–GC distance and Δ_{GC} is the GC–scattering region separation (van Langevelde et al. 1992). Lazio & Cordes (1998a, 1998b) constrain this ratio to be $D_{GC}/\Delta_{GC} \approx 50$, so that an extragalactic source seen through this scattering region should have a diameter of at least $75''$ at 1 GHz.

In their analysis, Lazio & Cordes (1998a, 1998b) paid particular attention to the source G359.87+0.18. First identified by Isaacman (1981; source 35W44) and Yusef-Zadeh & Morris (1987; source J), G359.87+0.18 was initially (and tentatively) classified as extragalactic by Anantharamaiah et al. (1991, p. 280). Their identification of this source as extragalactic was based on its compact morphology and flux density of 0.58 Jy at 0.33 GHz. This extragalactic classification was further strengthened by 8.5 and 15 GHz observations by W. M. Goss & K. R. Anantharamaiah (1990, unpublished) showing the source to have a FR II radio galaxy morphology with a $4''$ separation between components.

Based on 0.33 and 1.4 GHz images of the source, Lazio & Cordes (1998a) pointed out that the source could not be extragalactic and affected by the hyperstrong scattering region responsible for the enhanced angular broadening of Sgr A* and the OH masers. They suggested that the source might be an X-ray–quiet version of a Galactic jet source like 1E1740.7−2942 (Mirabel et al. 1992). Yusef-Zadeh, Cotton, & Reynolds (1998) have recently considered a number of classifications for the source including young supernova remnant, radio supernova, or nova remnant, based on high-resolution, total intensity images at 15 GHz and polarized intensity images at 5 GHz. They did not make an unambiguous classification but favored a young supernova remnant as most likely.

---

[1] NRC-NRL Research Associate.

[2] On leave from Raman Research Institute, Bangalore 560 080, India.

This paper reports new high-resolution images of G359.87+0.18 between 0.33 and 15 GHz and an H I absorption spectrum. We will conclude that the source is most likely an extragalactic source. In § 2 we present the new observations. In § 3 we summarize why we believe that G359.87+0.18 is likely to be extragalactic, § 4 discusses what this implies for the scattering region in the GC, and in § 5 we present our conclusions. Throughout we assume that the Galactic center is at distance of 8.5 kpc, implying that $1' = 2.5$ pc. We also use the convention that the spectral index α is given by $S \propto \nu^\alpha$.

2. SUMMARY OF OBSERVATIONS

Our observations of the source G359.87+0.18 span 0.33–15 GHz. Some of the observations are new, while in other cases we have reanalyzed existing data to obtain higher resolutions or dynamic ranges. Table 1 is our observing log. A summary of lower resolution observations of G359.87+0.18 is contained in Lazio & Cordes (1998a).

Image analysis was within AIPS using standard reduction procedures except where noted. We discuss each frequency separately.

2.1. *0.33 GHz*

As part of a search for radio pulsars in the GC, we observed Sgr A* at 0.33 GHz with the VLA in the A configuration. The radio pulsar survey will be described elsewhere (Lazio et al. 1998). The FWHM primary beam of the VLA at 0.33 GHz is 2°.5, which is large enough that little primary beam attenuation occurs over the 15′ distance between Sgr A* and G359.87+0.18. However, at 0.33 GHz the VLA can no longer be considered coplanar, and the standard assumption of a two-dimensional Fourier transform relation between the measured visibilities and the sky brightness distribution is no longer valid (Cornwell & Perley 1992).

We imaged G359.87+0.18 using the program DRAGON within NRAO's[3] Software Development Environment. Rather than attempt to image the entire primary beam, DRAGON allows small portions of the sky to be imaged

(Cornwell & Perley 1992). For each small image patch DRAGON inserts an appropriate phase shift, thereby restoring the validity of the assumption of coplanar baselines. Figure 1 shows the image patch containing G359.87+0.18 and the thread G359.79+0.17 to the south.

At 0.33 GHz G359.87+0.18 appears as a single, resolved component. Below we shall identify the appearance at 0.33 GHz as due partially to scattering.

The integrated flux density for G359.87+0.18 is 0.24 Jy. This value is only 40% of that determined by Anantharamaiah et al. (1991; 0.58 Jy) from VLA observations. This difference arises because we use data solely from the A configuration, while they used data from both A and B configurations. The B configuration is more compact than the A configuration, so the source is not as strongly resolved; the flux density reported by Anantharamaiah et al. (1991) is therefore more accurate.
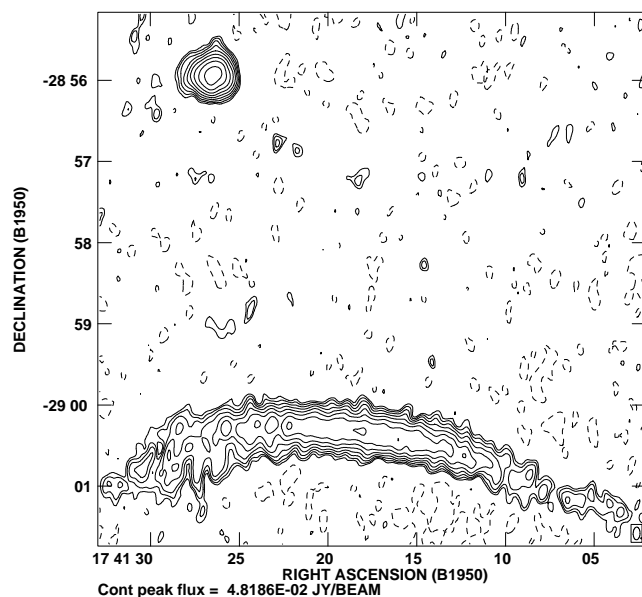

FIG. 1.—G359.87+0.18 and the nonthermal thread G359.79+0.17 at 0.33 GHz. The off-source noise level in the image is 1.2 mJy beam^{-1}, and the contour levels are -2.5, 2.5, 3.54, 5, 7.07, 10, 14.1, 20, ... mJy beam^{-1}. The beam is 9″.4 × 5″.1, with a position angle of $-2°$.

TABLE 1
VLA OBSERVING LOG FOR G359.87+0.18

Frequency (GHz)	Epoch	VLA Configuration	Observing Time	Beam (arcsec)	Image Noise Level (mJy beam^{-1})
0.33	1996 Oct 19	A	8 hr	9.4 × 4.3	1.7
1.5	1998 Mar 11	A	90 min.	2.5 × 1	0.58
8.5	1990 Oct 22	C	30 min.	5.7 × 2.4	0.11
	1998 Mar 11	A	15 min.	0.67 × 0.23	0.052
	1998 Apr 11	A[a]	90 min.	0.53 × 0.32	0.032
	all 1998 data	A	105 min.	0.51 × 0.30	0.028
	all data	...	2.25 hr	0.95 × 0.67	0.040
15	1990 Oct 22	C	30 min.	2.6 × 1.2	...
	1998 Apr 11	A[a]	4.5 hr	0.33 × 0.20	...
	1998 Apr 16	A	100 min.	0.32 × 0.15	...
	1998 Apr 23	A	70 min.	0.58 × 0.13	...
	all data	...	7.3 hr	0.38 × 0.16	0.049
H I........	1991 Oct 5–6	B, A	2 × 9 hr	4.7 × 3.6	...

[a] The VLA was in the A configuration, but only a 13 antenna subarray was used in the observations.

2.2. *1.5 GHz*

We observed G359.87+0.18 with the VLA at 1.42 and 1.66 GHz. The data from the two frequencies were calibrated separately and combined before imaging. Figure 2 shows the resulting image.

G359.87+0.18 consists of three nearly collinear components. In keeping with the nomenclature of Yusef-Zadeh et al. (1998), the stronger component to the northeast is component A, the central component is component B, and the faint, previously unrecognized component to the southwest is component C. While nearly collinear, the source is asymmetric, with component C at a larger distance from component B than is component A. Component C is also resolved with an extension pointing toward the two other components, while components A and B are, at best, only slightly resolved. The apparent connection between components A and B is an artifact of the beam, $2''.5 \times 1''$.

2.3. *8.5 GHz*

We observed G359.87+0.18 for 105 minutes on 1998 March 11 and April 11 with the VLA. All three components were detected. Furthermore, in the images from both days, component B showed a faint jetlike feature pointing toward component A. There was no variation either in the structure or in the flux density of the components between 1998 March 11 and April 11. Figure 3a shows the high-resolution image of G359.87+0.18 formed by combining the observations from these two epochs.

We also reprocessed a lower resolution, 30 minute observation of G359.87+0.18 acquired with the VLA on 1990 October 12. Figure 3b shows the image formed by combining all data from the 1990 and 1998 observations. The lower resolution data are more sensitive to extended structure, and component C is now more easily detected.

2.4. *15 GHz*

We acquired a total of 7 hr of observation on G359.87+0.18 in 1998 April with the VLA. The images

Fig. 3a

Fig. 3b

FIG. 3.—G359.87+0.18 at 8.5 GHz. (*a*) The high-resolution image formed from the 1998 observations. The off-source noise level in the image is 28 μJy beam^{-1}, and contours are $-0.1, 0.1, 0.141, 0.2, 0.283, 0.4, ...$ mJy beam^{-1}. The beam is shown in the lower left. (*b*) The lower resolution image formed by combining all data from observations in 1990 and 1998. The off-source noise level in the image is 40 μJy beam^{-1}, and contours are $-0.05, 0.05, 0.071, 0.1, 0.141, 0.2, ...$ mJy beam^{-1}. The beam is shown in the lower left.

made from the individual observations show only components A and B. There is no variation in the structure on the 3 days. We also reprocessed a lower resolution, 30 minute observation of G359.87+0.18 acquired with the VLA on 1990 October 12.

Figure 4 shows the image produced from the combined 1990 and 1998 data. Component A is resolved into two subcomponents, with one of the two being edge-brightened. The line joining the two subcomponents is at an angle of 70° to the axis of the large-scale morphology. Component B remains unresolved, but the jetlike feature is no longer present, indicating that it has a steep spectrum. We find a spectral index of $\alpha < -2.8$, although with considerable uncertainty ($\approx 20\%-30\%$). Our estimate for the flux density of the jet at 8.5 GHz may be contaminated by flux from the central part of component B, which would make the spectrum of the jet appear to be steeper than it actually is.

2.5. *H I Absorption Spectrum*

We reanalyzed VLA archive H I absorption spectra made toward Sgr A* (Plante, Lo, & Crutcher 1991). G359.87+0.18 is sufficiently close to Sgr A* that the primary beam attenuation is approximately 50%, and the delay beam attenuation is not significant. Thus we were able to obtain a spectrum for both G359.87+0.18 and Sgr
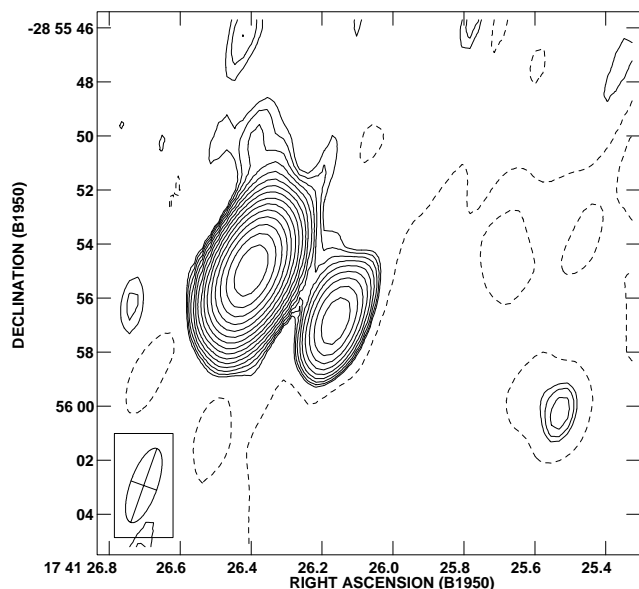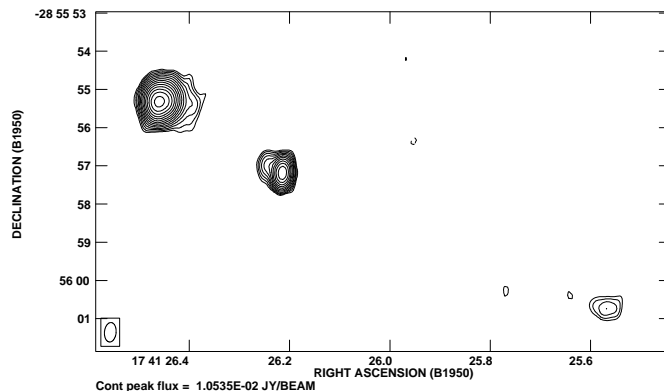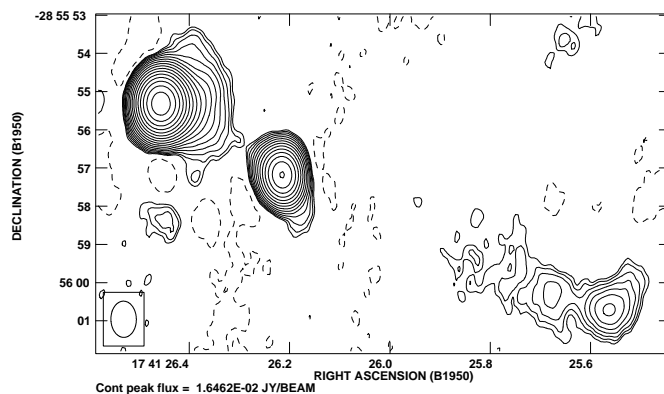

FIG. 2.—G359.87+0.18 at 1.5 GHz. This image was formed by combining data acquired at 1.42 and 1.66 GHz. The off-source noise level in the image is 0.59 mJy beam^{-1}, and contours are $-0.5, 0.5, 0.707, 1, 1.41, 2, ...$ mJy beam^{-1}. The beam is shown in the lower left.
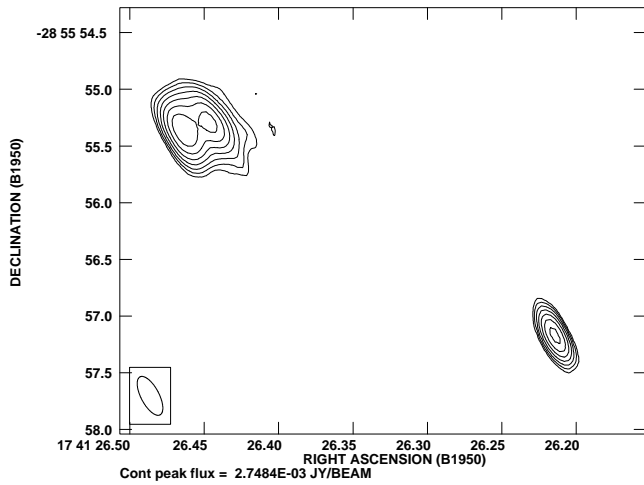
FIG. 4.—G359.87+0.18 at 15 GHz. This image was formed by combining all data from observations in 1998 April. Component C was not detected. The off-source noise level in the image is 49 μJy beam^{-1}; contours are $-0.25, 0.25, 0.354, 0.5, 0.707, 1, 1.41, 2, ...$ mJy beam^{-1}. The beam is shown in the lower left.

A*. The spectra toward these two sources are shown in Figure 5.

The -50 ("3 kpc arm") and $+40$ km s^{-1} features are seen in both spectra. Absorption is also seen at 0 km s^{-1} toward both sources, but the width of the absorption line is about twice as wide toward G359.87+0.18 as it is toward Sgr A* (40 km s^{-1} vs. 20 km s^{-1}). The large width of the 0 km s^{-1} gas toward G359.87+0.18 is similar to that seen toward B1739$-$298 ($\ell = 358°.92, b = 0°.07$), an extragalactic source approximately $1°$ away from Sgr A* (Dickey et al. 1983). In both cases the large width of the gas at 0 km s^{-1} may be a blend of two components, one centered near 0 km s^{-1} and the other near -20 km s^{-1}. The gas at -20 km s^{-1} does not appear in the spectrum of Sgr A* and presumably lies beyond Sgr A*.

3. IDENTIFICATION OF G359.87+0.18 AS AN FR II RADIO GALAXY

We classify G359.87+0.18 as extragalactic, most likely an FR II radio galaxy. Our classification is motivated by four criteria: morphology, spectrum, polarization, and lack of structural or flux density variation. We have also been able to place crude limits on the distance to the source that are consistent with it being extragalactic.

3.1. Morphology

The source clearly shows the morphology of an FR II source. Our 1.5 and 8.5 GHz images (Figs. 2 and 3b) show two components (A and C) surrounding a central component (B), which we identify as the core of the source. Our highest resolution, 15 GHz image (Fig. 4) resolves component A into two subcomponents, one of which is possibly an edge-brightened hot spot. At 8.5 GHz, component C is elongated in the direction toward component B, and component B has a steep-spectrum, jetlike feature pointed toward component A (Fig. 3a). The source is asymmetric; the separation between components A and B is 4″, and the separation between components B and C is 9″. This asymmetry could reflect a number of effects: the orientation of
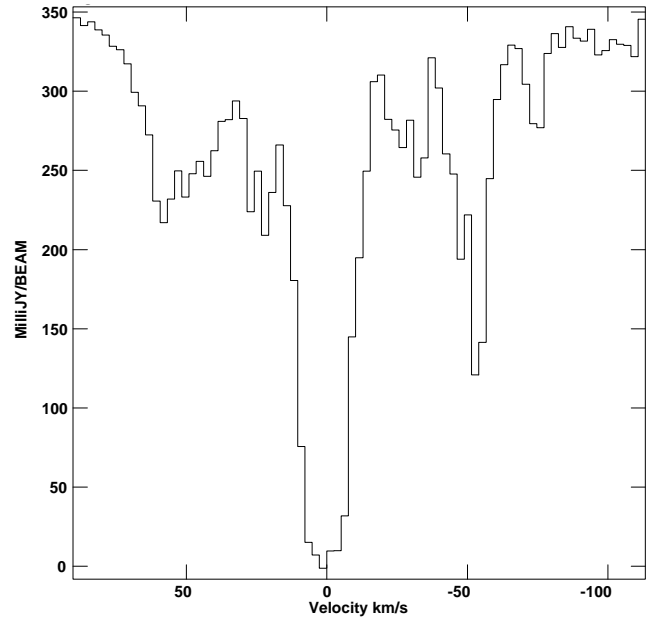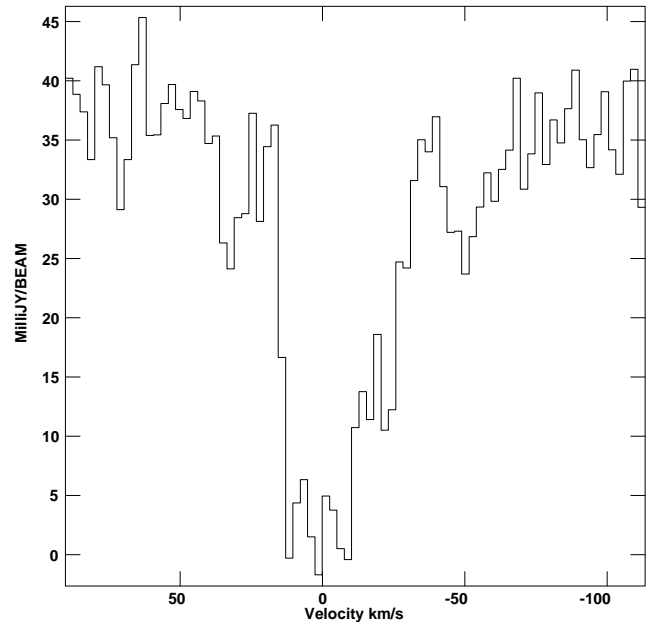

Fig. 5a

Fig. 5b

FIG. 5.—(a) H I absorption spectrum toward Sgr A*. (b) H I absorption spectrum toward G359.87+0.18. Both spectra have a velocity resolution of 2.6 km s^{-1}.

the source with respect to the line of sight, inhomogeneities in the ambient medium, and precession of the jet. A denser medium surrounding component A might also explain why it is considerably brighter than component C.

Within component A the line joining the two hot spots is oriented at an angle of approximately $70°$ to the line joining components A and B. Such misalignment is a common feature of FR II radio galaxies and is thought to result from changes in the jet orientation (Carilli & Barthel 1996).

3.2. Spectrum

At frequencies higher than 1.5 GHz, all components of G359.87+0.18 have extremely steep spectra, $\alpha \lesssim -1$.
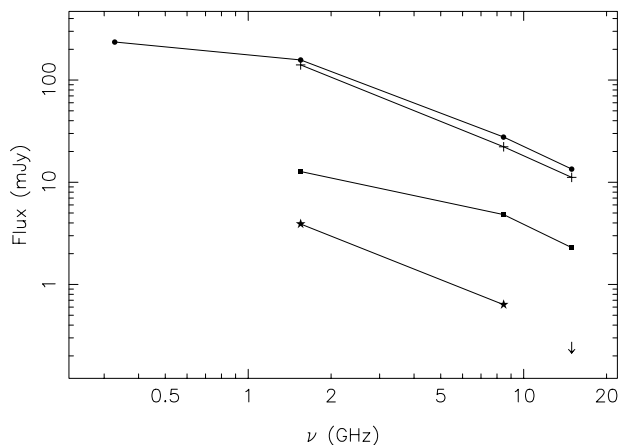
LAZIO ET AL.

FIG. 6.—Spectra of components of G359.87 + 0.18 as derived from the observations reported in this paper. Crosses indicate flux density measurements of component A, filled squares are for component B, and stars are for component C. At 15 GHz only an upper limit can be placed on the flux density of component C. Filled circles show the combined flux density for all three components; at 0.33 GHz the individual components cannot be distinguished.

Figure 6 shows the spectra of the individual components and of the entire source as derived from our measurements, and Table 2 tabulates the flux density of the components. Over the frequency range 1.5–15 GHz, component A has a spectral index of -1.1, component B has a spectral index of -0.7, and, between 1.5 and 8.5 GHz, component C has a spectral index of -1.1. At 15 GHz we can place only an upper limit (5 σ) of 0.24 mJy on the flux density of component C, which is slightly lower than that expected by an extrapolation of its spectrum, 0.3 mJy. Using Anantharamaiah et al.'s (1991) value for the 0.33 GHz flux density of 0.58 Jy and assuming that all three components contribute to the flux at 0.33 GHz, the spectrum flattens between 0.33 and 1.5 GHz with $\alpha \approx -0.8$.

Although our flux density measurements at different frequencies were obtained from observations with differing resolutions—with the exception of the 0.33 GHz observations (§ 2.1)—the components are sufficiently compact that this should introduce little error. In order to verify that this is the case, we have compared flux density measurements made at 8.5 GHz, determined both with and without the 1990 observations. The lower resolution 1990 observations should be more sensitive to extended flux that might be missed in our higher resolution 1998 observations. We find that the flux density measurements, determined with and without the 1990 observations, agree to within 10% for both components A and B.

TABLE 2

FLUX DENSITY OF G359.87 + 0.18 COMPONENTS

Frequency (GHz)	A (mJy)	B (mJy)	C (mJy)	Total (mJy)
0.33	...	...	...	236
1.55	141	12.7	3.9	157
8.5	22.2	4.82	0.63	27.7
15	11.2	2.29	<0.24	13.5

Yusef-Zadeh et al. (1998) used matched resolution, nearly simultaneous observations to find $\alpha_A = -1.6$ and $\alpha_B = -1.3$ for components A and B, respectively, between 5 and 15 GHz. Lazio & Cordes (1998a) find $\alpha_A \approx -1$ for component A over the frequency range 0.33–15 GHz, although they used flux density measurements made at differing resolutions at different epochs and assumed that component A was responsible for all of the flux at 0.33 GHz (see § 4.1).

Radio sources with $\alpha < -1$ belong to the class of ultra-steep spectrum (USS) sources (Röttgering et al. 1994). Members of this class include distant radio galaxies, head-tail galaxies, galaxy-cluster radio halos, "fading" radio galaxies, and pulsars. Of these, G359.87 + 0.18 is most likely to be a distant radio galaxy; it does not have the morphology of a head-tail galaxy, both radio halos and fading radio galaxies are quite rare, and the lack of variation (see below) indicates that it is probably not Galactic. In addition to its spectrum, G359.87 + 0.18 has two other characteristics typical of USS, distant radio galaxies (Röttgering et al. 1994). First, the majority of USS sources consist of more than one component, with 10% being triples. Second, the 12″ separation between components A and C is comparable with the median angular size of USS radio sources: for USS radio sources having a 0.33 GHz flux density of 0.5 Jy, the median angular size at 1.4 GHz is approximately 10″.

An extrapolation of the high-frequency spectrum of G359.87 + 0.18 to 0.33 GHz predicts a flux density of 0.8 Jy, which is in contrast to the observed value of 0.58 Jy (Anantharamaiah et al. 1991). We can identify both intrinsic and extrinsic causes for such a high-frequency steepening of the source's spectrum. The intrinsic cause would be a depletion of the high-energy electrons responsible for the synchrotron emission. This depletion could result from effects such as inverse Compton losses from the radiation field of the central engine (e.g., Blundell & Lacy 1995) or from a higher cosmic background radiation field at earlier epochs (e.g., Carilli et al. 1998). The extrinsic cause would be free-free absorption in the GC. An optical depth of $\tau \approx 0.3$ at 0.33 GHz would be sufficient to account for this difference. Optical depths $\tau \gtrsim 1$ at 0.33 GHz are seen elsewhere in the GC, e.g., near the radio arch (Anantharamaiah et al. 1991), and an extended, low-density H II region covers the inner degree or so of the GC (Mezger & Pauls 1979; Anish Roshi & Anantharamaiah 1997; see also § 4.3). From our limited spectral coverage of the source's spectrum, however, we cannot distinguish between these various possibilities.

3.3. Polarization

Yusef-Zadeh et al. (1998) show that the edge-brightened areas in component A are significantly polarized (6%–16%) at 5 GHz. This level of polarization is consistent with that seen in the lobes of FR II radio galaxies.

Because of large Faraday rotation, the intrinsic magnetic field direction within component A cannot be determined. From two closely spaced frequencies near 5 GHz, Yusef-Zadeh et al. (1998) derive a Faraday rotation measure of 3000 rad m^{-2}. Comparable Faraday rotation measures are seen along other lines of sight to the GC (Inoue et al. 1984; Tsuboi et al. 1985; Yusef-Zadeh & Morris 1987; Gray et al. 1995; Yusef-Zadeh, Wardle, & Parastaran 1997), and some FR II radio galaxies are embedded within a magnetized intracluster medium that could contribute to additional Faraday rotation (Carilli & Barthel 1996).

3.4. *Variability*

Our observations, combined with those summarized in Lazio & Cordes (1998a), provide a 10–15 yr time span over which G359.87+0.18 has been observed between 0.33 and 15 GHz. On short timescales (between a few days to a month) the source shows no structural variations, and the flux density is essentially constant. The angular resolution of many of the older observations (Lazio & Cordes 1998a) was not as high as in the present observations, so a detailed comparison of the structure of the source at different epochs is not possible. Components A and B have been detected, at approximately the same angular separation from each other, since 1986. Flux density comparisons are also hampered by the differing resolutions at the various different epochs. Nonetheless, the flux density of the source does not appear to have varied by more than 10% at any frequency over this time span, and flux density variations of roughly 10% may be the result of (extrinsic) refractive scintillation (Rickett, Coles, & Bourgois 1984).

3.5. *Distance*

We can place only crude limits on the distance to G359.87+0.18, but these are consistent with it being extragalactic. The H I spectra of G359.87+0.18 and B1739−298 are similar: both are dominated by an absorption feature centered approximately on 0 km s^{-1} with a considerable width, 40 km s^{-1}, and optical depth, $\tau \geq 2$. In both sources there is a suggestion that this large width is the superposition of two velocity components, one centered on 0 km s^{-1} and the other at −20 km s^{-1}. The 20 km s^{-1} gas does not appear in the spectrum of Sgr A* and presumably lies beyond it. The forbidden velocities near the GC make determining a distance from a rotation curve problematic, but the spectrum of G359.87+0.18 indicates that it is at least as far away as the GC and is consistent with an extragalactic distance.

We can also place a lower limit on the distance to G359.87+0.18 by requiring that its power output be consistent with that of other FR II galaxies. Extrapolating the (high-frequency) spectrum of G359.87+0.18 to 0.178 GHz, we find that its flux density would be 1.7 Jy. In order for its luminosity to exceed the break between FR I and FR II galaxies at 2×10^{25} W Hz^{-1} sr^{-1}, G359.87+0.18 must be at a distance of $D > 300$ Mpc ($z > 0.1$ for $H = 100$ km s^{-1} Mpc^{-1} and $q = \frac{1}{2}$).

By comparison with other USS distant radio galaxies, a redshift of $z \gtrsim 2$ is indicated (Röttgering et al. 1994). In a sample of high-redshift radio galaxies selected on the basis of $z > 2$, Athreya et al. (1997) find that most of them have unresolved cores with spectra $\alpha < -0.5$, which is similar to that of component B.

4. SCATTERING TOWARD THE GALACTIC CENTER

4.1. *Diameter and Shape of G359.87+0.18*

Figure 7 shows an 8.5 GHz image superposed on a 0.33 GHz image of G359.87+0.18. In contrast to its triple morphology at higher frequencies, G359.87+0.18 consists of a single component at 0.33 GHz that is approximately 20″ in diameter.

The structure of G359.87+0.18 at 0.33 GHz is due in part to radio-wave scattering. The alternative, that it reflects *only* the intrinsic structure of the source, seems unlikely. The high-frequency spectrum of G359.87+0.18, extrapo-
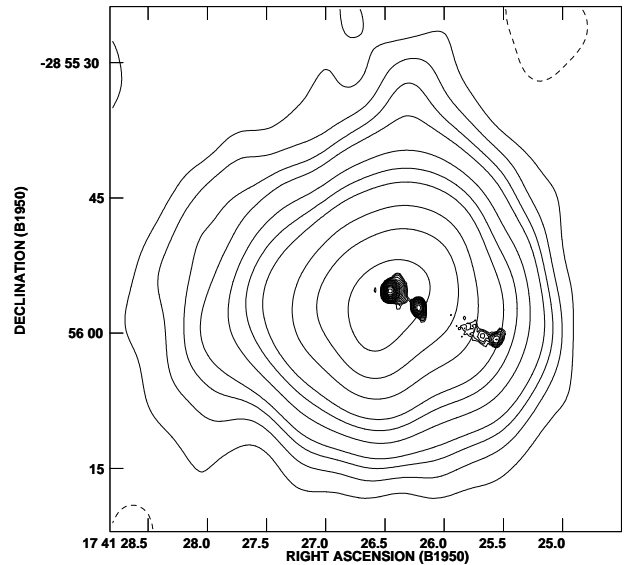

FIG. 7.—Comparison of the structure of G359.87+0.18 at 0.33 and 8.5 GHz. The 8.5 GHz contour levels are as in Fig. 3b; the 0.33 GHz contours are −2, 2, 4, 6, 8, 12, 16, 20, 28, 36, and 44 mJy beam^{-1}.

lated to 0.33 GHz and combined with modest free-free absorption, can account for the flux density of G359.87+0.18 (§ 3.2). If the 0.33 GHz structure is a halo, then the spectra of the individual components must flatten considerably or turn over below 1 GHz. While some spectral flattening is seen for USS sources, typically this occurs at frequencies below 0.1 GHz (Röttgering et al. 1994). Also, the halo would have to have a spectral index steeper than the individual components to avoid detection in our observations (§ 2) and those of Lazio & Cordes (1998a).

We cannot rule out the possibility that a halo contributes to the 0.33 GHz structure, however. Some FR II galaxies have low-frequency halos that surround the lobes (Carilli & Barthel 1996). A halo enclosing components A and C (separation 12″) would be largely resolved out by our observations; such a halo could have also escaped detection in the observations summarized in Lazio & Cordes (1998a), because either the previous observations were less sensitive than those reported here or they did not have sufficient angular resolution. The uncertainty in the amount of free-free absorption along this line of sight also allows for the existence of a halo. We require an optical depth of $\tau \approx 0.3$ to reconcile the observed and expected flux densities (§ 3.2). An optical depth only slightly larger, $\tau = 0.5$, for instance, would permit a halo with a 0.33 GHz flux density of $S_\nu \approx 0.1$ Jy to exist while remaining consistent with the observed flux density.

Lazio & Cordes (1998a) considered the scattering properties of G359.87+0.18 assuming that the 0.33 GHz structure represented only the contribution from component A. In fact, all three components will contribute to the 0.33 GHz structure. The observed diameter of a source at a particular frequency can be modeled as the quadrature sum of the intrinsic diameter and the scattering diameter. It is assumed commonly that scattering affects the apparent diameter of only relatively compact sources. However, if the scattering diameter is comparable with that of the intrinsic diameter,

then the apparent diameter of the source will reflect the contribution from scattering, *even if* the intrinsic structure of the source is not compact (Cohen & Cronyn 1974).

In solving for the scattering diameter of G359.87+0.18, we will obtain a range of allowed values because of our limited information about its intrinsic structure at 0.33 GHz. The observed diameter of G359.87+0.18 at 0.33 GHz is 19″. We first obtain an upper limit on the scattering diameter by assuming that component A, which dominates the flux density of the source at high frequencies, continues to dominate at 0.33 GHz. Component A has a high-frequency diameter (assumed to be intrinsic) of approximately 2″. Assuming that the intrinsic diameter is frequency independent, we find a scattering diameter of $\theta_s \leq 19''$. We obtain an approximate lower limit on the scattering diameter by taking the 12″ separation between components A and C to be characteristic of the 0.33 GHz intrinsic diameter. In this case $\theta_s \gtrsim 14''$. The equivalent range on the 1 GHz scattering diameter is 1″.5–2″.

While large, the scattering diameter of G359.87+0.18 is not unusually so, nor is it unique toward the GC. The nearby extragalactic sources B1739−298 and B1741−312 ($\ell = 357°.87$, $b = -1°$) have similar lines of sight through the entire disk of the Galaxy. Their diameters indicate that they are heavily scattered but not affected by the hyperstrong region in front of Sgr A* (Lazio & Cordes 1998b). Their scattering diameters, scaled to 0.33 GHz, are roughly 6″, which is only a factor of 2–3 smaller than that inferred for G359.87+0.18.

The shape of the image at 0.33 GHz is also *irregular*. We characterize the image shape as irregular as opposed to anisotropic because the image displays a "mottled" or "lumpy" appearance (Fig. 7). The intrinsic structure, as inferred from the high-frequency observations, contributes little to the irregular appearance. We have convolved our 1.5 GHz image (Fig. 2) with a circular Gaussian scattering disk 15″ in diameter. The resulting image is comparable in size with that of our 0.33 GHz image but is considerably smoother.

Our lack of knowledge about the low-frequency, intrinsic structure of G359.87+0.18 limits the extent to which we can explain this irregular appearance. This appearance is probably the result of both the intrinsic structure at 0.33 GHz and anisotropic scattering. Observations at frequencies between 0.33 and 1.4 GHz would be useful in separating these effects. Unfortunately, existing observations in this frequency range do not have sufficient angular resolution even to resolve the source (e.g., the 0.84 GHz Molonglo Observatory Synthesis Telescope survey had a beam of 90″ × 45″; Gray 1994).

4.2. Uniform versus Patchy Scattering Region

Using a likelihood analysis of the OH maser scattering diameters and source counts of extragalactic sources toward the GC, Lazio & Cordes (1998b) concluded that the characteristic separation between Sgr A* and the GC scattering region is 150 pc, that the scattering region is centered on $(\ell, b) = (0°, 0°)$, and that its extent in Galactic longitude is between ±0°.5 and ±1°. As a consequence, Sgr A* and the heavily broadened OH masers are seen through a hyperstrong scattering region that covers at least a portion of the GC. The implied scattering diameter at 0.33 GHz is 12″ for a Galactic source and at least 600″ for an extragalactic source. In this section we consider three pos-

sibilities that would allow G359.87+0.18 to be both extragalactic and not heavily scattered.

The first possibility is that the hyperstrong scattering region is a relatively homogeneous region of sufficiently limited angular extent that it does not cover G359.87+0.18. While the scattering region's extent in Galactic latitude is poorly constrained (Lazio & Cordes 1998b), we now show that if the scattering region is homogeneous, it almost certainly extends to at least the Galactic latitude of G359.87+0.18. The maser OH 359.762+0.120 is 7′.4 south of G359.87+0.18 and has an anisotropic scattering disk of 1″.2 × 0″.36 at 1.6 GHz (Frail et al. 1994). The nonthermal thread G0.08+0.15 is 13′ northeast of G359.87+0.18, and its width may be affected by scatter broadening (Anantharamaiah et al. 1991). The nonthermal thread G359.79+0.17 is 4′.7 south of G359.87+0.18 (Fig. 1), and as we now show, its width is also likely to be affected by scatter broadening. From a 1.4 GHz image provided by C. C. Lang (1998, private communication), we have determined that the width of the thread varies from 12″ to 19″; an example is shown in Figure 8. At this frequency the expected scattering diameter for a Galactic source affected by the hyperstrong scattering region is 0″.6, so we consider these widths to be the intrinsic widths of the thread. As was noted above, the expected scattering diameter for a Galactic source at 0.33 GHz is 12″. If we assume that the intrinsic width is frequency independent and add the intrinsic width and scattering diameter in quadrature, the expected width of the thread should vary between 17″ and 22″. In fact, the observed width of the thread at 0.33 GHz varies between 23″ and 29″.

We regard the agreement between the expected and observed widths of the thread as evidence that scattering affects the thread G359.79+0.17. The modest discrepancies between the expected and observed width can be resolved by a combination of a frequency-dependent intrinsic width and a larger separation between the thread and scattering region than assumed. A frequency-dependent intrinsic width would arise if the synchrotron-emitting electrons responsible for the thread have a greater transverse extent at low energies (Anantharamaiah et al. 1991). The expected scattering diameter depends on the distance between the source and the scattering region. We have taken the scattering diameter to be that of Sgr A*, which is appropriate if the thread G359.79+0.17 is also 150 pc behind the scattering region (Lazio & Cordes 1998b). If the thread is more distant, its expected scattering diameter is

$$\theta_s \simeq \theta_{\text{Sgr A*}} \frac{\Delta}{\Delta_{\text{Sgr A*}}}, \qquad (1)$$

where $\theta_{\text{SgrA*}}$ is the scattering diameter of Sgr A*, $\Delta_{\text{SgrA*}}$ is the Sgr A* scattering-region separation, and Δ is the thread scattering-region separation. If the thread G359.79+0.17 is 100 pc more distant than Sgr A*, scattering alone could explain the discrepancy between the observed and expected widths of the thread.

Therefore, if the scattering region is homogeneous and covers the GC uniformly, it extends to a Galactic latitude of at least 0°.18. Since G359.87+0.18 does not display the expected enhanced broadening, we conclude that the scattering region is unlikely to be homogeneous.

The second possibility is that the scattering region is patchy or clumpy and that there are "holes" in it. If so, the
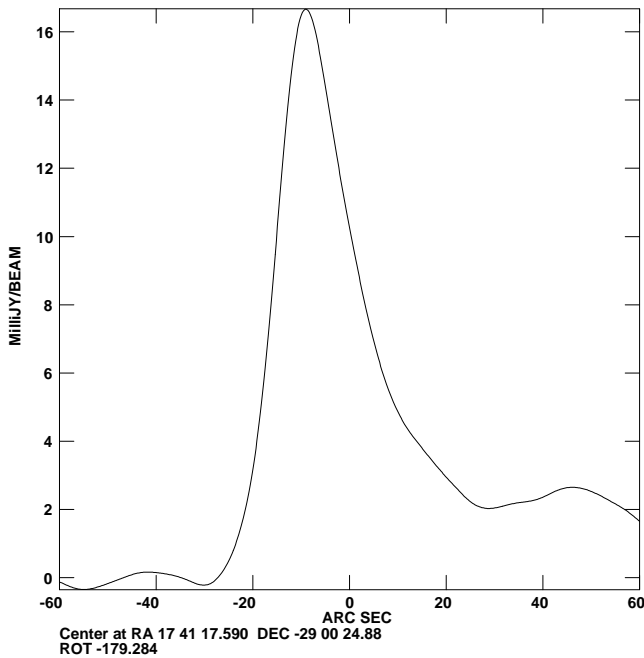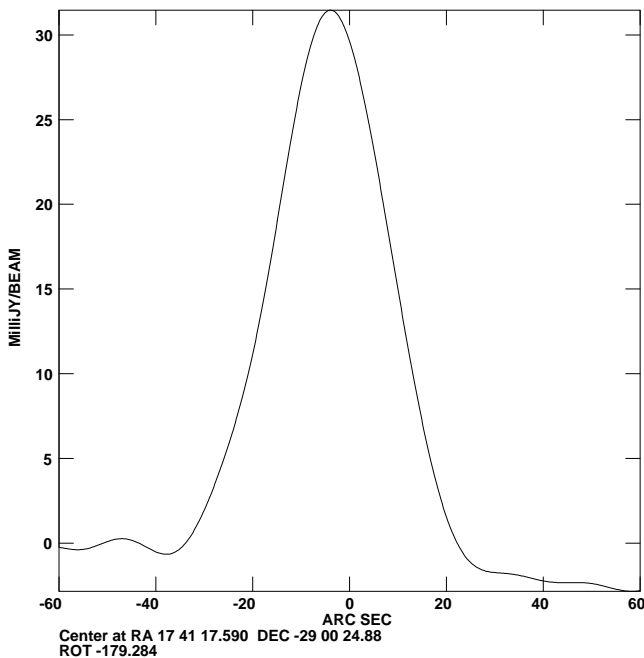
Fig. 8a

Fig. 8b

FIG. 8.—Two cross cuts perpendicular to the major axis of thread G359.79+0.17. (a) 1.4 GHz. (b) 0.33 GHz; this cut was formed from the image shown in Fig. 1.

size of the clumps would have to be smaller than the 4″7 separation between G359.87+0.18 and the thread G359.79+0.17, which is equivalent to 12 pc at the GC.

A scattering region composed of clumps would also explain the contrasts between the diameters of OH 0.190+0.036 and OH 0.319−0.040 and of Sgr A OH 1720:B and Sgr A OH 1720:C. The (1.6 GHz) scattering diameter of OH 0.190+0.036 is only 0″1 (van Langevelde & Diamond 1991), whereas OH 0.319−0.040 has a scattering diameter of 1″2 (Frail et al. 1994) even though it is only 9′ away and (angularly) more distant from Sgr A*. The case

of OH 0.190+0.036 is not as clear-cut as that of G359.87+0.18, however, because OH 0.190+0.036 could be just behind or in front of the scattering region. While we cannot establish definitely that OH 0.190+0.036 is close to the GC, there are two indications that this is likely. First, in order for it to be unaffected by the scattering region, OH 0.190+0.036 would have to be at least 100 pc closer to the Sun than Sgr A* (i.e., no more than 50 pc behind the scattering region). Its projected distance from Sgr A* is 30 pc. OH/IR stars in the GC have a volume density that varies as r^{-2} and a distribution that is centered on Sgr A* (Lindqvist, Habing, & Winnberg 1992a). Therefore, it is 10 times more likely for an OH/IR star to be 30 pc distant from Sgr A* than it is to be 100 pc distant. Second, OH/IR stars show a ℓ-v diagram indicative of circular rotation about the center (Lindqvist et al. 1992a). The radial velocity of OH 0.190+0.036 (+159 km s^{-1}; Lindqvist et al. 1992b) is not only consistent with that expected from circular rotation but is actually larger than the value predicted by Lindqvist et al.'s (1992a) model. A radial velocity larger than the model value is exactly what is expected if most of the source's velocity is projected along the line of sight, i.e., if OH 0.190+0.036 is at its projected distance from Sgr A*.

Sgr A OH 1720:B is a collection of 1720 MHz OH maser features in Sgr A West having anisotropic angular diameters with major axes of approximately 0″85. Sgr A OH 1720:C is an unresolved 1720 MHz OH maser located 15′ (≈ 35 pc) away and associated with Sgr A East (Yusef-Zadeh et al. 1999). In this case, Sgr A West is known to lie in front of Sgr A East (Pedlar et al. 1989). Thus if the scattering region covered the GC uniformly, Sgr A OH 1720:C would be expected to show a large scattering disk.

A third possibility for the scattering of G359.87+0.18 is that the scattering region is far from Sgr A* (greater than 1 kpc). We do not consider this option to be viable. In their likelihood analysis of the scattering region toward the GC, Lazio & Cordes (1998b) found that even if they assumed G359.87+0.18 to be extragalactic, there was still a deficit of sources near Sgr A* requiring the scattering region to be closer than 500 pc to the GC. (Their analysis also implicitly assumed a relatively homogeneous scattering region.) Moreover, their likelihood analysis of the OH maser scattering diameters, which was independent of any extragalactic sources, indicated that the Sgr A* scattering-region separation is between 50 and 300 pc. Nonetheless, the scattering diameter of G359.87+0.18 is formidable, 1″5–2″ at 1 GHz. This diameter is comparable with that seen for other heavily scattered sources in the Galaxy (e.g., 1849+005, Fey, Spangler, & Cordes 1991; NGC 6634B, Moran et al. 1990). Since the mean free path for intersecting a comparable region of scattering is 8 kpc (Cordes et al. 1991), there is a good chance there could be additional scattering contributed by a region on the far side of the Galaxy.

4.3. Implications for the Scattering Region

We therefore conclude that the scattering region is inhomogeneous or clumpy on scales of 10–20 pc. Prevailing models for the scattering region explain the scattering as arising in the ionized outer layers of molecular clouds, which are produced either from photoionization by the hot stars in the GC (Yusef-Zadeh et al. 1994) or as an evaporative interface between the molecular clouds and the ambient X-ray gas (Lazio & Cordes 1998b). Inhomogeneities in the scattering region on scales of 10–20 pc are

consistent with a molecular cloud origin: molecular clouds in the GC also have scale sizes of 10–20 pc (Güsten 1989).

We have examined CO ($J = 1 \to 0$, Bally et al. 1987; $J = 2 \to 1$, Oka et al. 1998) ℓ-v diagrams of the GC in an effort to identify a "gap" in the molecular cloud distribution through which G359.87+0.18 could shine. We focus on CO because its emission traces densities of $n \gtrsim 500$ cm^{-3}. Since typical molecular cloud central densities in the GC are $n \gtrsim 10^4$ cm^{-3}, CO will trace the outer layers of molecular clouds, the regions that can be ionized easily. In addition, high-resolution, sensitive surveys exist for these transitions, with resolutions comparable with that which we infer for the separation between scattering clumps. The $J = 1 \to 0$ observations had a 100″ beam (=4 pc at the distance of the GC); the $J = 2 \to 1$ observations had a 9′ beam (=20 pc).

The distribution of molecular clouds in the GC displays a well-known asymmetry, with a concentration of molecular material toward $\ell > 0°$. This asymmetry means that a hole in the scattering region for $\ell < 0°$ is quite plausible. Indeed, perhaps more difficult to explain is the enhanced angular broadening toward the threads G359.79+0.17 and OH 359.762+0.120, since there do not appear to be obvious GC molecular clouds in these directions. The molecular cloud(s) (and the associated ionized outer layers) responsible for the enhanced broadening toward the threads G359.79+0.17 and OH 359.762+0.120 may have velocities near 0 km s^{-1}. Most GC molecular clouds can be identified because they have large velocities. Some GC molecular clouds do have velocities near 0 km s^{-1}, however, and these clouds can be confused with gas along the line of sight to the GC.

We distinguish between the *outer scale* in the scattering region and the *separation* between scattering clumps. The outer scale, l_0, is simply the largest scale on which the density fluctuations responsible for radio-wave scattering occur. If the density fluctuations arise from a turbulent process, the outer scale reflects the largest scale on which turbulent energy is injected. If the scattering arises in the ionized outer layers of molecular clouds (Yusef-Zadeh et al. 1994; Lazio & Cordes 1998b), the outer scale presumably is comparable with the thickness of these ionized layers. In both models the outer scale is small, $l_0 \lesssim 10^{-4}$ pc, but it is not necessarily related to the separation between individual clouds.

The small outer scale (and high temperature; Lazio & Cordes 1998b) of the scattering region (or cloudlets) means that it contributes little to the free-free emission and absorption toward the GC. Rather, the bulk of the free-free emission and absorption would be contributed by the extended low-density H II region (Mezger & Pauls 1979; Anish Roshi & Anantharamaiah 1997). This extended low-density H II region may be (partially) responsible for the scattering disks of G359.87+0.18, B1739−298, and B1741−312. The hyperstrong scattering seen toward Sgr A* and various OH masers is due to this clumpy GC scattering region.

5. CONCLUSIONS

We have presented new observations of the source G359.87+0.18 at frequencies between 0.33 and 15 GHz and an H I absorption spectrum. We conclude that this source is a FR II radio galaxy, based on the following characteristics.

Morphology.—The source is a collinear triple source, with the northeast component being edge brightened, the central component having a jetlike feature pointing toward the northeast component, and the southwest component being extended toward the central component.

Polarization.—The edge-brightened component shows a fractional polarization of approximately 10%.

Spectrum.—The source has a steep spectrum, with a spectral index of $\alpha < -1$, which is characteristic of high-redshift galaxies.

Variability.—No significant structural or flux density variations have been observed over short (few weeks to a month) or long (10–15 yr) timescales.

Steep-spectrum radio galaxies are typically at $z \gtrsim 2$. We have not been able to determine a distance to the source, but the H I absorption spectrum we have presented suggests a lower limit of 25 kpc, and the classification as an FR II radio galaxy suggests a lower limit to the redshift of 0.1.

Although G359.87+0.18 is only 15′ from Sgr A*, it is not affected by the hyperstrong scattering region that is responsible for the large diameter of Sgr A*. If it were, G359.87+0.18 would have a diameter in excess of 600″ at 0.33 GHz, in contrast to the observed diameter of 20″. We attribute the lack of hyperstrong scattering toward G359.87+0.18 to an inhomogeneous scattering region. An inhomogeneous scattering region would also explain the small diameter of the masers OH 0.190+0.036 and Sgr A OH 1720:C, both of which appear to be seen through the region of enhanced scattering but have diameters less than 0″.1 at 1.6 and 1.7 GHz, respectively. The scattering region would have to be inhomogeneous on 5–10′ scales (10–20 pc at the Galactic center) in order to explain the small diameters of these two sources. This scale is comparable with the scale of molecular clouds in the GC. Prevailing models explain the hyperstrong scattering as due to ionized regions on the surfaces of molecular clouds. We regard the close correspondence between the size of molecular clouds and the inhomogeneities in the scattering region as evidence for a connection between the two.

REFERENCES

Anantharamaiah, K. R., Pedlar, A., Ekers, R. D., & Goss, W. M. 1991, MNRAS, 249, 262
Anish Roshi, D., & Anantharamaiah, K. R. 1997, MNRAS, 292, 63
Athreya, R. M., Kapahi, V. K., McCarthy, P. J., & van Breugel, W. 1997, MNRAS, 289, 525
Backer, D. C., Zensus, J. A., Kellermann, K. I., Reid, M., Moran, J. M., & Lo, K. Y. 1993, Science, 262, 1414
Bally, J., Stark, A. A., Wilson, R. W., & Henkel, C. 1987, ApJS, 65, 13
Blundell, K. M., & Lacy, M. 1995, MNRAS, 274, L9
Bower, G. C., & Backer, D. C. 1998, ApJ, 496, L97
Carilli, C. L., & Barthel, P. D. 1996, A&A Rev., 7, 1
Carilli, C. L., Röttgering, H. J. A., Miley, G. K., Pentericci, L. H., & Harris, D. E. 1998, in The Most Distant Radio Galaxies, ed. H. J. A. Röttgering, P. N. Best, & M. D. Lehnert (Amsterdam: North-Holland), in press
Cohen, M. H., & Cronyn, W. M. 1974, ApJ, 192, 195
Cordes, J. M., Weisberg, J. M., Frail, D. A., Spangler, S. R., & Ryan, M. 1991, Nature, 354, 121
Cornwell, T. J., & Perley, R. A. 1992, A&A, 261, 353
Davies, R. D., Walsh, D., & Booth, R. S. 1976, MNRAS, 177, 319
Dickey, J. M., Kulkarni, S. R., van Gorkom, J. H., & Heiles, C. 1983, ApJS, 53, 591
Fey, A. L., Spangler, S. R., & Cordes, J. M. 1991, ApJ, 372, 132
Frail, D. A., Diamond, P. J., Cordes, J. M., & van Langevelde, H. J. 1994, ApJ, 427, L43
Gray A. D. 1994, MNRAS, 270, 822
Gray, A. D., Nicholls, J., Ekers, R. D., & Cram, L. E. 1995, ApJ, 448, 164
Güsten, R. 1989, in The Center of the Galaxy, ed. M. Morris (Dordrecht: Kluwer), 89
Inoue, M., Takahashi, T., Tabara, H., Kato, T., & Tsuboi, M. 1984, PASJ, 36, 633
Isaacman, R. 1981, A&AS, 43, 405
Krichbaum, T. P., et al. 1993, A&A, 274, L37
Lazio, T. J. W., & Cordes, J. M. 1998a, ApJS, 118, 201
Lazio, T. J. W., & Cordes, J. M. 1998b, ApJ, 505, 715
Lazio, T. J. W., Cordes, J. M., Kassim, N. E., & Arzoumanian, Z. 1998, in preparation
Lindqvist, M., Habing, H. J., & Winnberg, A. 1992a, A&A, 259, 118
Lindqvist, M., Winnberg, A., Habing, H. J., & Matthews, H. E. 1992b, A&AS, 92, 43
Mezger, P. G., & Pauls, T. 1979, in The Large-Scale Characteristics of the Galaxy, ed. W. B. Burton (Dordrecht: Reidel), 357
Mirabel, I. F., Rodríguez, L. F., Cordier, B., Paul, J., & Lebrun, F. 1992, Nature, 358, 215
Moran, J. M., Rodríquez, L. F., Greene, B., & Backer, D. C. 1990, ApJ, 348, 150
Oka, T., Hasegawa, T., Hayashi, M., Handa, T., & Sakamoto, S. 1998, ApJ, 493, 730
Pedlar, A., Anantharamaiah, K. R., Ekers, R. D., Goss, W. M., van Gorkom, J. H., Schwarz, U. J., & Zhao, J. 1989, ApJ, 342, 769
Plante, R. L., Lo, K. Y., & Crutcher, R. M. 1991, ApJ, 445, L113
Rickett, B. J., Coles, W. A., & Bourgois, G. 1984, A&A, 134, 390
Rogers, A. E. E., et al. 1994, ApJ, 434, L59
Röttgering, H. J. A., Lacy, M., Miley, G. K., Chambers, K. C., & Saunders, R. 1994, A&AS, 108, 79
Tsuboi, M., Inoue, M., Handa, T., Tabara, H., & Kato, T. 1985, PASJ, 37, 359
van Langevelde, H. J., & Diamond, P. J. 1991, MNRAS, 249, 7
van Langevelde, H. J., Frail, D. A., Cordes, J. M., & Diamond, P. J. 1992, ApJ, 396, 686
Yusef-Zadeh, F., Cotton, W. D., & Reynolds, S. P. 1998, ApJ, 498, L55
Yusef-Zadeh, F., Cotton, W., Wardle, M., Melia, F., & Roberts, D. A. 1994, ApJ, 434, L63
Yusef-Zadeh, F., & Morris, M. 1987, ApJ, 320, 545
Yusef-Zadeh, F., Roberts, D. A., Goss, W. M., Frail, D. A., & Green, A. J. 1999, ApJ, 512, in press
Yusef-Zadeh, F., Wardle, M., & Parastaran, P. 1997, ApJ, 475, L119